Phys. Rev. C56, 812-824 (1997),

PROPERTIES OF THE HYPOTHETICAL SPHERICAL SUPERHEAVY NUCLEI

ROBERT SMOLAŃCZUK*

Sołtan Institute for Nuclear Studies
Hoża 69, PL-00-681 Warszawa, Poland
and
Gesellschaft für Schwerionenforschung
D-64291 Darmstadt, Germany

(Received 7 April 1997)

Abstract

Theoretical results on the ground–state properties of the hypothetical spherical superheavy atomic nuclei are presented and discussed. Even–even isotopes of elements $Z = 104 - 120$ are considered. Certain conclusions are also drawn for odd–A and odd–odd superheavy nuclei. Results obtained earlier for even–even deformed superheavy nuclei with $Z = 104 - 114$ are given for completeness.

Equilibrium deformation, nuclear mass, alpha–decay energy, alpha–decay half–life, dynamical fission barrier, as well as spontaneous–fission half–life are considered. Beta–stability of superheavy nuclei is also discussed. The calculations are based on the macroscopic–microscopic model. A multidimensional deformation space describing axially–symmetric nuclear shapes is used in the analysis of masses and decay properties of superheavy nuclei.

We determined the boundaries of the region of superheavy nuclei which are expected to live long enough to be detected after the synthesis in a present–day experimental set–up.

PACS number(s): 25.85.Ca, 23.60.+e, 21.10.Dr, 27.90.+b

* e–mail address: smolan@fuw.edu.pl

I. INTRODUCTION

In the last years considerable effort, both theoretical [1–21] and experimental [22–36], has been devoted to investigation of superheavy atomic nuclei, *i.e.* the very heavy nuclei which exist, or are expected to exist, only due to shell effects. Since the potential energy calculated in a macroscopic model (*i.e.* a model without any shell effects) forms a very small barrier or even no barrier for these nuclei [37], without these effects superheavy nuclei would decay practically immediately. Both theoretical and experimental investigations were concentrated on the nuclei expected from theoretical considerations to be deformed and, therefore, called "deformed superheavy nuclei".

Our theoretical results obtained so far [2–6] have led to the prediction of enhanced stability against spontaneous fission and alpha decay for nuclei close to the not yet observed nucleus $^{270}108_{162}$ ($^{270}\mathrm{Hs}_{162}$). According to theoretical considerations, this system should have features of the deformed doubly magic nucleus [38–40,2]. The prediction of increased stability of nuclei close to $^{270}108_{162}$ ($^{270}\mathrm{Hs}_{162}$) [2–6] has been supported by the joint Dubna–Livermore experiment [22–27]. These results opened new prospects for the synthesis and investigation of properties of deformed superheavy nuclei, not only the physical properties but also the chemical ones, because some predicted half–lives exceed one second which is nowadays the lower limit for radiochemical investigations [41].

Comparison of the calculated spontaneous–fission and alpha–decay half–lives [3,4] have led to the conclusion that the alpha–decay mode should dominate for even–even nuclei with $Z \geq 108$ and the neutron number around $N = 162$ at which the deformed neutron shell is expected [38–40,2]. Although the calculations of Refs.[3,4] have been performed for even–even nuclei, the same conclusion is expected to hold for odd–A and odd–odd deformed superheavy nuclei with $Z \geq 107$ and N close to 162. This is because the spontaneous–fission half–life increases considerably due to the effect of an unpaired nucleon [42] while the alpha–decay half–life is much less sensitive to this effect [43]. The prediction of the dominance of the alpha decay for nuclei with $Z \geq 107$ and $N \approx 162$ has been supported by experiments carried out at GSI–Darmstadt, where new elements $Z = 110$ [28,29], 111 [30] and 112 [31] have been produced. The synthesized nuclei $^{269}110_{159}$, $^{271}110_{161}$, $^{272}111_{161}$ and $^{277}112_{165}$ decayed by the emission of the alpha–particle after time of the order of $0.1 - 1$ ms. The discovery of the new elements became possible when a level of detection sensitivity of 1 pb had been reached due to an upgrade of the experimental set–up at GSI–Darmstadt

[44].

A theoretical advance [1–6] has been achieved due to a proper description of spontaneous–fission half–lives and alpha–decay energies for deformed superheavy nuclei. The calculations of spontaneous–fission half–lives based on the macroscopic–microscopic method have been performed dynamically [45,46], *i.e.* the fission trajectory has been determined by the minimization of the action integral in a multidimensional deformation space. A metric in this space is defined by the tensor of inertia, calculated within the cranking model, which takes into account the shell structure of a nucleus [47]. Resistance of a nucleus against shape changes, connected with the motion along the one–dimensional trajectory L in a multidimesional deformation space, is described by the effective inertia. The latter quantity is defined as $B \equiv B(\alpha_i^L(s)) = \sum_{jk} B_{\alpha_j\alpha_k}(\alpha_i^L(s))\frac{d\alpha_j^L(s)}{ds}\frac{d\alpha_k^L(s)}{ds}$, where α_i denotes i–th deformation parameter, $B_{\alpha_j\alpha_k}(\alpha_i^L(s))$ is the component of the tensor of inertia, and the parameter s specifies the position of a point on the trajectory L. Effective inertia is more reliable than a phenomenological mass parameter. The latter has been applied in earlier static calculations, exploiting a trajectory along which the potential energy is minimal [48–51,10]. The phenomenological mass parameter has at least one free parameter fitted to experimental data and disregards the shell structure of a nucleus.

In the dynamical calculations of the spontaneous–fission half–lives [1–4] for deformed superheavy nuclei both the macroscopic–microscopic potential energy and the tensor of inertia have been calculated individually for each nucleus. No averaging over proton and neutron numbers has been used. A big enough deformation space has been applied. A four–dimensional deformation space describing axially and reflection–symmetric shapes of nuclei has been used. Larger deformation space leads to a larger potential energy barrier. This is due to a stronger potential energy lowering around the equilibrium point than at the top of the barrier [1]. A value of 0.7 MeV was taken as the average zero–point vibration energy in the fission degree of freedom [1].

Nuclear masses and, consequently, alpha–decay energies, have been calculated by means of the macroscopic–microscopic method in the four–dimensional deformation space. Three of five parameters [6,52], appearing in terms independent of deformation, have been readjusted to recent experimental data [53] for even–even nuclei with $Z \geq 82$ and $N \geq 126$. This readjustment was necessary because we used a larger deformation space than the ones applied in other macroscopic–microscopic calculations of nuclear masses [54,40,11].

In Refs.[50,51], short spontaneous–fission half–lives have been obtained in static calculations, taking the nucleus $^{258}Fm_{158}$ as a model for heavier nuclei and assuming that the trajectory behind the fission barrier is short with the emerging fragments being nearly spherical and close to the doubly magic nucleus $^{132}Sn_{82}$. The calculations [50,51] give no enhencement of fission stability near the deformed shell at $N = 162$ and are inconsistent with the data obtained in the joint Dubna–Livermore experiment [22–27].

Earlier static calculations [48,49,10] have been performed in a smaller deformation space than the one applied presently, using the phenomenological mass parameter, and with the averaging of the potential energy of a nucleus over N and Z numbers. A smaller deformation space, the potential energy and the effective inertia averaging over N and Z have also been used in earlier dynamical calculations [55]. These simplifications produce large errors because the effective inertia and potential energy of a nucleus appear in the exponential in the formula for the spontaneous–fission half–life and, therefore, they should be determined as precise as possible.

Besides our calculations [1–6] based on the macroscopic–microscopic theory, various macroscopic–microscopic models [7–15], the extended Thomas–Fermi with Strutinsky–integral (ETFSI) theory [16], the fermion dynamical symmetry model (FDSM) [17] and the self–consistent Hartree–Fock–Bogoliubov (HFB) [18,19], Hartree–Fock (HF) [20] and relativistic mean field (RMF) [21] methods have also been applied recently in order to describe various properties of known superheavy nuclei and also the "traditional" ones which are unobserved so far.

The traditional superheavy nuclei are expected to be spherical and are located on the nuclear chart around a spherical doubly magic nucleus next to $^{208}Pb_{126}$. According to the considerations based on the Woods–Saxon single–particle potential, $^{298}114_{184}$ is a spherical doubly magic superheavy nucleus [56]. The same conclusion has been drawn from an independent investigation [57] based on a non–local potential. This prediction is also supported by the recent RMF calculations [58,21]. However, different results were obtained in Ref.[20] by means of the HF method with the SkP variant [59] of the Skyrme interaction. In the latter case a larger proton magic number $Z = 126$ was obtained and the nucleus $^{310}126_{184}$ was predicted [20] to be the spherical doubly magic one next to $^{208}Pb_{126}$. Also the calculations performed in Ref.[19] by means of the HFB method with the non–local Gogny force [60] indicate that $Z = 114$ is not a magic number. Moreover, calculations exploiting the FDSM model predict the region of spherical (or deformation soft) superheavy nuclei around the nucleus $^{278}114_{164}$ for which they give the minimal shell correction to the nuclear mass [17].

Our calculations [3–6] based on the macroscopic–microscopic theory support the suggestion made in Ref.[49] that spherical superheavy nuclei probably do not form an "island" on the nuclear chart, separated from the "peninsula" of known nuclei by a region of deep instability, as it was believed earlier, *e.g.* [61–65]. Now we expect that, due to the stabilization effect of the deformed shells at $Z = 108$ and $N = 162$, the peninsula of known nuclei should extend up to the island of spherical superheavy nuclei. In other words, the deformed superheavy nuclei located around the unobserved nucleus $^{270}108_{162}$ ($^{270}\mathrm{Hs}_{162}$), and the spherical ones, situated in the neighbourhood of the nucleus $^{298}114_{184}$, constitute a continuation of this paninsula on the nuclear chart. However, a completely different conclusion has been drawn recently from the study [17]. According to the calculations [17] based on the FDSM model, the newly discovered nuclei $^{269}110_{159}$ [28], $^{271}110_{161}$ [29], $^{272}111_{161}$ [30] and $^{277}112_{165}$ [31] are in the true island of spherical superheavy nuclei which is shifted downward in neutron number.

Many spherical superheavy nuclei discussed in the present paper are located in, or close to, the area of beta–stability and, therefore, alpha decay and spontaneous fission are the main decay modes for these nuclei. However, for those spherical superheavy nuclei which are situated outside the area of beta–stability, and which have very large alpha–decay and spontaneous–fission half–lives, beta decay may dominate [66].

In Ref.[18], the approximate proton– and neutron–drip lines have been determined by using the spherical HFB method with the SkP variant [59] of the Skyrme interaction. The even–even superheavy nuclei for which we obtained alpha–decay and spontaneous–fission half–lives greater than 1 μs in Ref.[4] and in the present paper are located on the nuclear chart between these lines, close to the proton–drip line. Calculations performed in Ref.[16] by using the ETFSI theory also indicate that these nuclei are proton stable. The analysis performed in Ref.[20] by means of the deformed HF+SkP method shows that some superheavy nuclei for which we calculate alpha–decay and spontaneous–fission half–lives greater than 1 μs are proton–unstable. However, their alpha–decay half–lives are much smaller than the corresponding half–lives with respect to proton emission and, therefore, the proton emission does not influence the total half–lives. The value of 1 μs is presently a lower limit for measurements of the half–life of a superheavy nucleus after its synthesis [67].

In forthcoming experiments the synthesis of spherical superheavy nuclei is planned.

Using both stable target and beam it is not possible to form the compound nucleus very close to the spherical doubly magic $^{298}114_{184}$, *i.e.* the one with $N \approx 184$. Therefore, the nuclei with $Z \approx 114$ and with the largest possible numbers of neutrons are to be produced [68]. A possibility of the production of nuclei very close to the spherical doubly magic one may appear in the near future due to the use of the neutron–rich radioactive ion beams [69].

The aim of this study is to present theoretical results on the ground–state properties calculated for spherical isotopes of elements $Z = 104 - 120$. For this purpose we use the model [1,4,6] which had some success in reproducing and predicting the ground–state decay properties of deformed superheavy nuclei [2–6]. In the present work we consider nuclear mass, ground state to ground state alpha–decay properties: alpha–decay energy and half–life, as well as spontaneous–fission properties: dynamical fission barrier and spontaneous–fission half–life. Theoretical results on the decay properties obtained earlier for deformed superheavy nuclei with $Z = 104 - 114$ [4] are also given for completeness. Moreover, beta–stability of elements $Z = 104 - 120$ is discussed. The calculations are performed for even–even nuclei. Certain conclusions are also drawn for odd–A and odd–odd superheavy nuclei. The results on alpha–decay energy and alpha–decay half–life for some spherical superheavy nuclei given in the present paper have been shown in Refs.[5,6] and the results on the spontaneous–fission properties of spherical isotopes of the element 104 have been presented in Ref.[70]. In Refs.[5,6,70], reflection–asymmetric shapes of heaviest isotops of elements $104 - 110$ have been disregarded. Reflection asymmetry of these nuclei is taken into account in the present calculations.

In Section II, description of the calculation is given. Calculated properties of superheavy nuclei are presented and discussed in Section III. Conclusions are drawn in Section IV.

II. DESCRIPTION OF THE CALCULATION

The superheavy nuclei are expected to be axially and reflection–symmetric or spherical in their ground states. The reflection asymmetry at the ground state appears for lighter nuclei around Radium and Barium [71,72] and for very few heaviest isotopes of elements $104 - 110$. We expect that the deformed superheavy nuclei are also axially and reflection–symmetric during tunneling through the potential energy barrier. This result has been obtained in Ref.[1] as a consequence of the dynamical treatment of the spontaneous fission, *i.e.* finding a one–dimensional fission trajectory which minimizes the action integral in a multidimensional deformation space. Large effective inertia obtained for trajectories with nuclear shapes with broken axial or reflection symmetry prevent a fissioning nucleus from admitting such shapes [1]. The reflection asymmetry is important only for very few deformed isotopes of the element 104 in which it removes the small second hump of the potential energy barrier [73]. The axial asymmetry of fissioning spherical and transitional superheavy nuclei has been discussed in Ref.[74]. According to the results obtained in Ref.[74], the inclusion of non–axial shapes in the description of the tunneling through the potential energy barrier plays some role only for very few nuclei considered in the present paper. For the reasons given above we only take into account the axially and reflection–symmetric shapes in the analysis of the ground–state decay properties of superheavy nuclei. We describe these shapes in the intrinsic frame of reference by the standard even–multipolarity deformation parameters β_λ, $\lambda = 2, 4, 6, 8$, appearing in the expression for the nuclear radius in terms of spherical harmonics $Y_{\lambda 0}(\vartheta)$. The only exceptions are very few heaviest isotopes of elements $104 - 110$ for which reflection asymmetry must be taken into account. Equilibrium deformation and nuclear masses for these nuclei are calculated in the seven–dimensional deformation space $\{\beta_\lambda\}$, $\lambda = 2, 3, ..., 8$.

The potential energy of a nucleus and its dependence on deformation is calculated by using the macroscopic–microscopic method. This method consists in adding a correction, arising from shell effects, to the macroscopic part of the potential energy. The Yukawa–plus–exponential model [54] is used for the macroscopic energy. Parameters apearing in this model are taken from Ref.[54] with the exception of the volume–asymmetry parameter κ_V, the charge–asymmetry parameter $c_{\rm a}$ and the constant a_0 which are specified below. The instability in this model, discussed in Ref.[75], does not appear in our calculations because the largest deformation parameter used has the multipolarity $\lambda = 8$. The Yukawa–plus–exponential model becomes unstable in the region of actinide and transactinide nuclei for $\lambda > 12$.

The microscopic energy is obtained by means of the Strutinsky method [76]. The single–particle–energy levels are obtained by the diagonalization of the Woods–Saxon single–particle hamiltonian [77] in the deformed harmonic oscillator basis. A version of the Woods–Saxon hamiltonian with the “universal” values of the constants [77], applicable, on the average, throughout the periodic table, is used. This hamiltonian is diagonalized in the deformed–oscillator basis with 19 harmonic oscillator shells for both neutrons and protons. At a given deformation, 550 neutron and 350 proton lowest lying states are taken into account [40]. The residual pairing interaction is calculated by means of the usual BCS approximation with the strength taken from Ref.[40]. The potential energy is calculated individually for each nucleus, without any averaging over Z and N numbers.

In the analysis of the spontaneous fission we describe the inertia of a nucleus with respect to changes of deformation by the tensor of inertia which is calculated in the cranking approach with the inclusion of pairing interaction (formula IX.41a in Ref.[47]). We determine the fission trajectory and, consequently, the spontaneous–fission half–life in a dynamical way. It consists in a search for the dynamical fission trajectory $L_{\rm dyn}$ which fulfills the variational principle of the least–action. We use, instead of the full dynamics performed in the four–dimensional deformation space $\{\beta_\lambda\}$, $\lambda = 2, 4, 6, 8$, the simpler one proposed in Ref.[1] and exploited in Refs.[2–4]. It consists in a search for the dynamical fission trajectory $L_{\rm dyn}$ in a four–dimensional deformation subspace $\{\beta_2, \beta_4, \beta_6^{\rm m}, \beta_8^{\rm m}\}$, where $\beta_6^{\rm m}$ and $\beta_8^{\rm m}$ denote the values of the deformations β_6 and β_8, respectively, at which the potential energy $E(\beta_2, \beta_4; \beta_6^{\rm m}, \beta_8^{\rm m})$ is minimal at a given point (β_2, β_4). The simpler dynamics is a good approximation to the full one because higher multipolarity deformations β_6 and β_8 are generally small and change rather slowly along the fission trajectory, not increasing much the effective inertia of a nucleus.

Since the model cannot be solved analytically, it is necessary to calculate the potential energy and all components of the tensor of inertia on a grid in a multidimensional deformation space. In order to get a properly dense grid and to speed up the time–consuming calculations simultaneously, we calculate the potential energy and all components of the tensor of inertia on the so called "basic" grid and then we get the values of these quantities on a more dense grid by interpolating the respective values at the basic grid points by the third–order polynomials. We use the basic grid with the steps $\Delta\beta_2 = \Delta\beta_4 = 0.05$ and the final one with $\Delta\beta_2 = 0.01$ and $\Delta\beta_4 = 0.0025$, the same ones as in Ref.[4].

We apply the semiclassical WKB approximation to determine the probability of the penetration through the potential energy barrier along a one–dimensional fission trajectory in the four–dimensional deformation space $\{\beta_2, \beta_4, \beta_6^{\rm m}, \beta_8^{\rm m}\}$. The energy of a fissioning nucleus is taken as a sum of the equilibrium energy and the average value of the zero–point vibration energy in the fission degree of freedom (per one degree of freedom). We use the value of 0.7 MeV for the latter quantity for the reason discussed in Subsection III.C. The spontaneous–

fission half–lives for heaviest isotopes of elements $104-110$, $^{290-292}104$, $^{292-294}106$, $^{296}108$ and $^{298}110$, which are reflection–asymmetric in their ground states, are calculated along trajectories obtained in the four–dimensional deformation space $\{\beta_2,\beta_4,\beta_6^{\rm m},\beta_8^{\rm m}\}$ with the energy of each fissioning nucleus calculated relative to the equilibrium energy obtained in the seven–dimensional deformation space $\{\beta_\lambda\}$, $\lambda=2,3,...,8$. The equilibrium energy lowering for these nuclei, due to the inclusion of the odd–multipolarity deformations, is significantly smaller than 0.7 MeV.

In the calculations of nuclear masses, the volume–asymmetry parameter κ_V, the charge–asymmetry parameter $c_{\rm a}$ and the constant a_0 were refitted to 77 experimentally known masses [53] of even–even nuclei with $Z\geq 82$ and $N\geq 126$ because of the use of the larger (four–dimensional) deformation space than the ones used in other macroscopic–microscopic calculations [54,40,11]. The obtained values are:

$$\kappa_V=1.990\ ,\quad c_{\rm a}=0.572\ \mathrm{MeV}\ ,\quad a_0=11.0\ \mathrm{MeV}\ . \tag{1}$$

The alpha–decay energy Q_α for each nucleus is obtained by subtracting the theoretical mass of its daughter nucleus and the experimentally known mass of the alpha–particle from the theoretical mass of a decaying nucleus. We calculate the alpha–decay half–life T_α by means of the Viola and Seaborg formula [43] with parameters [5,6]:

$$a=1.81040\ ,\quad b=-21.7199\ ,\quad c=-0.26488\ ,\quad d=-28.1319\ , \tag{2}$$

adjusted to 58 even–even nuclei with $Z>82$ and $N>126$ for which both T_α and Q_α are measured [78]. Previous adjustments of a,b,c and d [43,79] were done for a much smaller number of nuclei in comparison to the present one.

III. RESULTS AND DISCUSSION

III.A Doubly magic superheavy nuclei

The proton and neutron single–particle–energy spectra for the well deformed $^{270}108_{162}$ ($^{270}\mathrm{Hs}_{162}$) and the spherical $^{298}114_{184}$ nuclei are shown in Fig.1. These spectra are obtained by means of the Woods–Saxon single–particle potential with the universal variant of parameters [77].

Large energy gaps, between $Z=114$ and 115 in the proton spectrum, and between $N=184$ and 185 in the neutron spectrum of the spherical nucleus $^{298}114_{184}$, both equal to 2.1 MeV, create large shells. Filling up of large nuclear shells by outer nucleons takes place in magic nuclei. Therefore, we expect that $^{298}114_{184}$ is the spherical doubly magic nucleus next to $^{208}Pb_{126}$.

Similar but smaller energy gaps are obtained for the not yet observed deformed nucleus $^{270}108_{162}$ ($^{270}Hs_{162}$), between $Z = 108$ and 109 in the proton spectrum and between $N = 162$ and 163 in the neutron spectrum [38–40,2]. The deformations of the multipolarities β_4 and β_8 for protons and β_4 and β_6 for neutrons contribute substantially to the creation of these gaps. Both the proton and neutron energy gaps are equal to 1.4 MeV. The effect of shell stabilization for the deformed nucleus $^{270}108_{162}$ ($^{270}Hs_{162}$) and for the neighbouring deformed ones leads to the appearence of an area of increased stability in the region where the deep instability was expected earlier, *e.g.* [61–65]. This area connects the peninsula of known nuclei with the hypothetical island of stability around $^{298}114_{184}$. Therefore, we call $^{270}108_{162}$ ($^{270}Hs_{162}$) "deformed doubly magic nucleus" as distinct from the "traditional" doubly magic one, $^{298}114_{184}$, which is expected to be spherical.

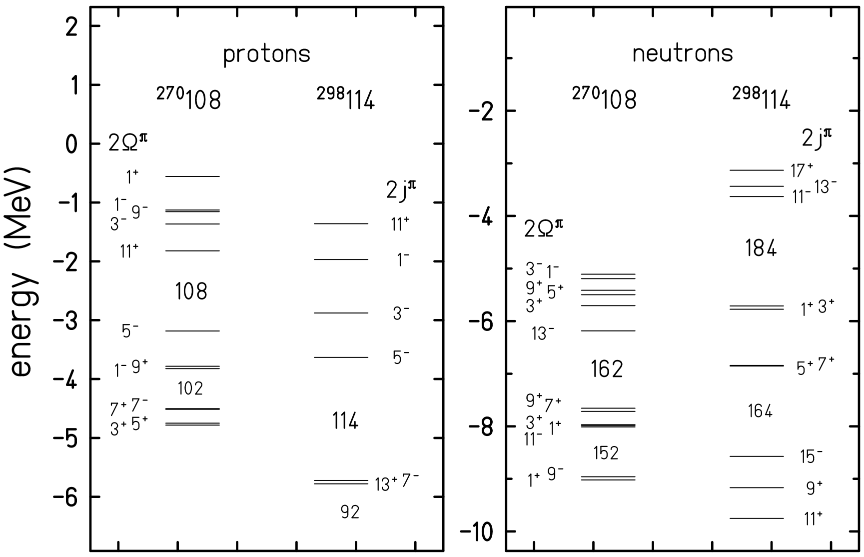

Fig.1. Proton and neutron single–particle–energy spectra calculated for the deformed $^{270}108_{162}$ ($^{270}Hs_{162}$) and spherical $^{298}114_{184}$ doubly magic superheavy nuclei. At each single–particle level the absolute value of the projection of spin Ω, multiplied by two, on the symmetry axis, together with state's parity π ($^{270}108_{162}$) or the state parity π with the spin j, multiplied by two ($^{298}114_{184}$), are indicated.

III.B Equilibrium deformation

The majority of the considered nuclei are prolate–shaped ($\beta_2^0 > 0$) or spherical ($\beta_2^0 \cong 0$). The oblate–shaped nuclei ($\beta_2^0 < 0$) are listed in Table I together with the prolate (spherical) – oblate energy difference. This table contains nuclei for which we calculate the alpha–decay and spontaneous–fission half–lives larger than 0.1 μs which is the value one order of magnitude less than the smallest half–life possible to measure after the synthesis of a superheavy nucleus in a present–day experimental set–up [67].

We indicate the scale of deformation of a nucleus by the deformation energy $E_{\rm def}$, defined as the difference between the energies at the spherical and the equilibrium shapes,

$$E_{\rm def}(Z,N) = E(Z,N,0) - E(Z,N,\beta_\lambda^0)\ . \tag{3}$$

Fig.2 shows a contour map of this quantity for prolate or spherical equilibrium shapes for even–even nuclei with $Z = 82 - 120$. We consider the nuclei with $E_{\rm def} \gtrsim 2$ MeV as well deformed. Most of nuclei with $Z = 82 - 120$ shown in Fig.2 are or are expected to be well deformed. The regions of spherical ($E_{\rm def} \approx 0$) and transitional ($E_{\rm def} \lesssim 2$ MeV) nuclei are located around the doubly magic nuclei $^{208}\text{Pb}_{126}$ and $^{298}114_{184}$. The unobserved nucleus $^{270}108_{162}$, as well as the superheavy nuclei synthesized so far, are predicted to be well deformed. It is also clearly seen in Fig.2 that the heaviest superheavy nucleus produced so far, $^{277}112_{165}$ [31], is located on the nuclear chart very close to the region of spherical superheavy nuclei. In this figure, the region of even–even spherical superheavy nuclei with both calculated alpha–decay and spontaneous–fission half–lives larger than 0.1 μs is shown.

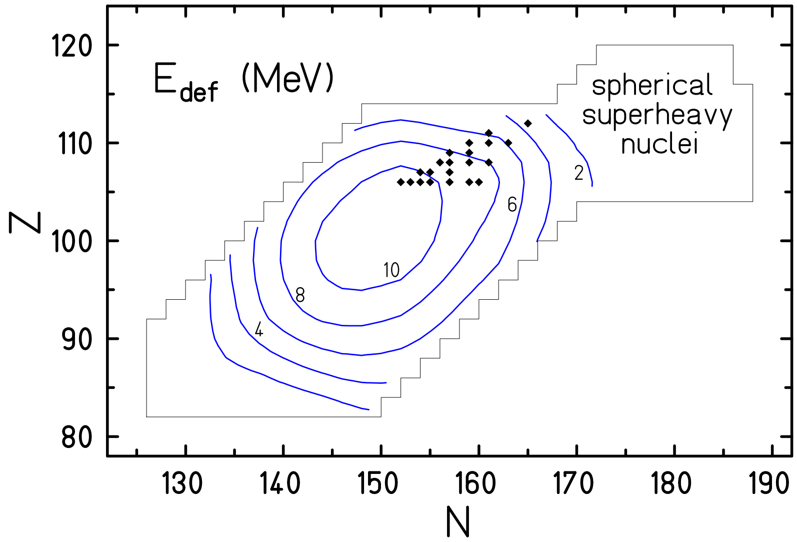

Fig.2. Contour map of the prolate (or spherical) equilibrium deformation energy $E_{\rm def}$ for even–even nuclei with the atomic number $Z = 82 - 120$. Numbers at contour lines give energy in MeV. The energy difference between neighbouring contour lines is equal to 2 MeV. Rhomb–shaped symbols denote the deformed superheavy nuclei with $Z \geq 106$ synthesized so far.

III.C Total shell correction energy

The total shell correction energy $E_{\rm sh}$, responsible for stabilization of superheavy nuclei, is defined as the difference between the total potential energy for the equilibrium shape and the macroscopic part of the potential energy for the spherical shape (zero deformation),

$$E_{\rm sh}(Z,N) = E(Z,N,\beta_\lambda^0) - E_{\rm macro}(Z,N,0)\,. \tag{4}$$

Since the spherical shape is the equilibrium point in the macroscopic (*i.e.* without shell structure) model, the total shell correction defined by Eq.(4) is the gain in energy of a nucleus due to its shell structure, including the effect of pairing.

Fig.3 shows a contour map of the total shell correction energy $E_{\rm sh}$ for prolate or spherical shapes of even–even nuclei with $Z = 82 - 120$. It is calculated for the same nuclei for which the deformation energy $E_{\rm def}$ is given in Fig.2. Both $E_{\rm def}$ and $E_{\rm sh}$ are obtained in the four–dimensional deformation space $\{\beta_\lambda\}$, $\lambda = 2, 4, 6, 8$, for all nuclei except the reflection–asymmetric ones around Radium [71] and $^{290-292}104$, $^{292-294}106$, $^{296}108$ and $^{298}110$. For the reflection–asymmetric nuclei, $E_{\rm def}$ and $E_{\rm sh}$ are obtained in the seven–dimensional deformation space $\{\beta_\lambda\}$, $\lambda = 2, 3, ..., 8$.

Three minima of $E_{\rm sh}$ in the considered region of nuclei are shown in Fig.3. The deepest one ($E_{\rm sh} = -14.32$ MeV) is obtained at the spherical doubly magic nucleus $^{208}{\rm Pb}_{126}$. The next one ($E_{\rm sh} = -7.15$ MeV) appears at the deformed doubly magic nucleus $^{270}108_{162}$. The last minimum has about the same depth ($E_{\rm sh} = -7.16$ MeV) as that at $^{270}108_{162}$. It is obtained at the nucleus $^{296}114_{182}$, which is very close to the spherical doubly magic one $^{298}114_{184}$. The minimum at $^{208}{\rm Pb}_{126}$ is the most steep, the one at $^{270}108_{162}$ is more shallow and the last one at $^{296}114_{182}$ is the most shallow.

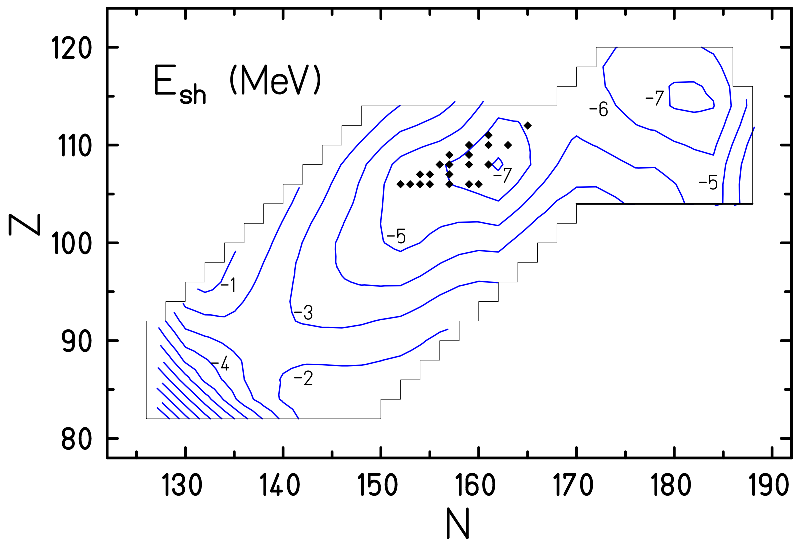

Fig.3. Contour map of the total prolate (or spherical) shell correction energy $E_{\rm sh}$ for even–even nuclei with $Z = 82 - 120$. Numbers at contour lines give energy in MeV. The energy difference between neighbouring contour lines is equal to 1 MeV. Rhomb–shaped symbols denote the deformed superheavy nuclei with $Z \geq 106$ synthesized so far.

The absolute value of 7.04 MeV for $E_{\rm sh}$ obtained for the spherical doubly magic $^{298}114_{184}$ is about two times smaller than that calculated for the spherical doubly magic $^{208}\mathrm{Pb}_{126}$ and close to the one for the deformed doubly magic $^{270}108_{162}$. Therefore, in the calculations of the properties of spherical superheavy nuclei we use a value of 0.7 MeV for the average zero–point vibration energy per one degree of freedom, the same one as in the case of deformed superheavy nuclei. However, a considerably larger value of the zero–point vibration energy than the average one may appear for the doubly magic nucleus $^{298}114_{184}$, as it is observed in the case of lighter spherical doubly magic nuclei. This possible significant increase of the zero–point vibration energy for the nucleus $^{298}114_{184}$ would decrease considerably its stability, as discussed in Subsection III.J.

III.D Nuclear mass and beta–stable superheavy nuclei

Mass of a nuclide is calculated as the mass excess, *i.e.* $(M(\text{in u}) - A)$, in MeV, where u is the atomic mass unit. The masses obtained for prolate or spherical equilibrium shapes, as well as the calculated decay properties discussed in the subsections below, are collected in Table II. They are listed for even–even isotopes of elements $Z = 104 - 120$ excluding the nuclei discussed in Ref.[4]. Only the results for nuclei with both calculated alpha–decay and spontaneous–fission half–lives larger than 0.1 μs are given.

Two minimal masses obtained for each isobaric chain of even–even nuclides with $A \geq 264$ determine beta–stable superheavy nuclei. This is because the neighbouring odd–odd isobars have larger masses. We found that the superheavy nuclei $^{264-274}104$, $^{268-280}106$, $^{276-286}108$, $^{282-292}110$, $^{288-298}112$, $^{294-302}114$ and $^{300-304}116$ should be beta–stable. However, there is a possibility of existence of more beta–stable superheavy nuclei because it may happen for some isobaric chains of even–even nuclei that for more than two nuclides with the smallest masses the neighbouring odd–odd isobares will have larger masses.

III.E Alpha–decay energy

The alpha–decay energy Q_α for elements $Z = 100 - 120$ as a function of neutron number N is shown in Fig.4. The effect of the spherical neutron shell at $N = 184$ and the weaker one of the deformed neutron shell at $N = 162$ are seen as minima of Q_α for particular elements at these neutron numbers. The effect of the spherical proton shell at $Z = 114$ manifests itself for nuclei with $N \approx 184$ as a larger gap between the curves describing Q_α versus N for $Z = 114$ and 116 in comparison to the gaps between other pairs of neighbouring curves.

This effect is comparable to that of the deformed proton shell at $Z = 108$ for nuclei with $N \approx 162$.

The experimentally known values for alpha–decay energy for even–even nuclei [78,23] are shown in Fig.4 together with the recently measured data for odd–N isotopes of the element 110, $^{269}110_{159}$ [28], $^{271}110_{161}$ [29] and $^{273}110_{163}$ [26]. The alpha–decay energy from a report [34] on the possible production of the isotope $^{267}110_{157}$ is also shown. In Fig.4, the increase of the experimental alpha–decay energy for the nucleus $^{273}110_{163}$ is against to the trend seen for the lighter isotopes of the element 110. This is in agreement with the tendency obtained for our calculated Q_α values and seems to confirm that the deformed neutron shell appears exactly at $N = 162$. In one of the two alpha–decay chains observed at GSI–Darmstadt after the synthesis of the nucleus $^{277}112_{165}$ [31], the alpha–decay energy of its doughter nucleus, which is again $^{273}110_{163}$, also shows the increse of the alpha–decay energy at $N = 163$ in agreement with the joint Dubna–Livermore experiment [26].

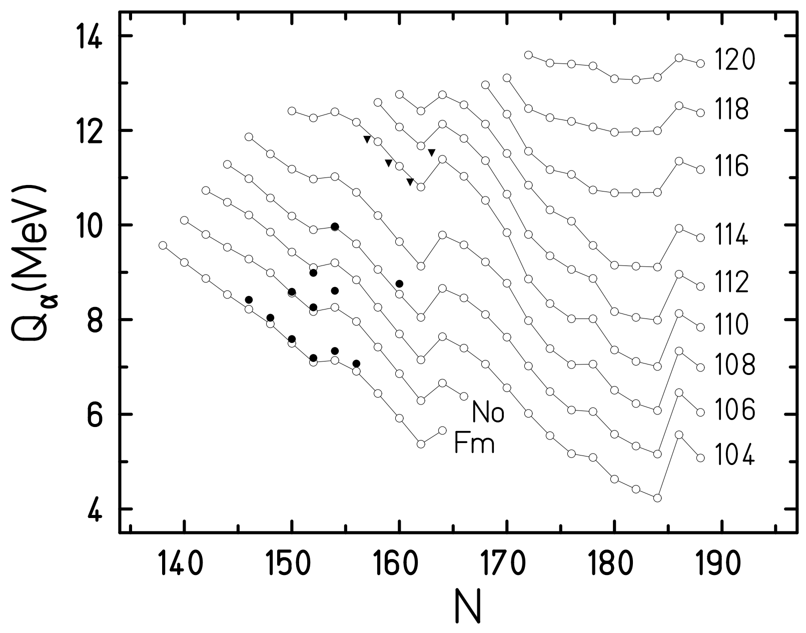

Fig.4. Calculated alpha–decay energy Q_α , in MeV, as a function of neutron number N, for elements 100 – 120. Experimental values taken from Refs.[78,23,26,28,29,34] are indicated by full circles, for even–even nuclei, and full triangles, for odd–N isotopes of the element 110.

III.F Alpha–decay half–life

Fig.5 shows logarithm of the alpha–decay half–life T_α as a function of neutron number N. It is calculated for the same nuclei for which the alpha–decay energy Q_α is given in Fig.4. The dependence of $\log_{10}T_\alpha(s)$ on Z and N is a consequence of the dependence of the alpha–decay energy Q_α on these quantities. Therefore, all shell effects seen in Q_α in Fig.4 are clearly reflected in $\log_{10}T_\alpha(s)$ in Fig.5. It is worth to stress that the alpha–decay half–life calculated for the spherical doubly magic nucleus $^{298}114_{184}$ (12 m) is not much larger than that obtained for the deformed doubly magic nucleus $^{270}108_{162}$ (6 s).

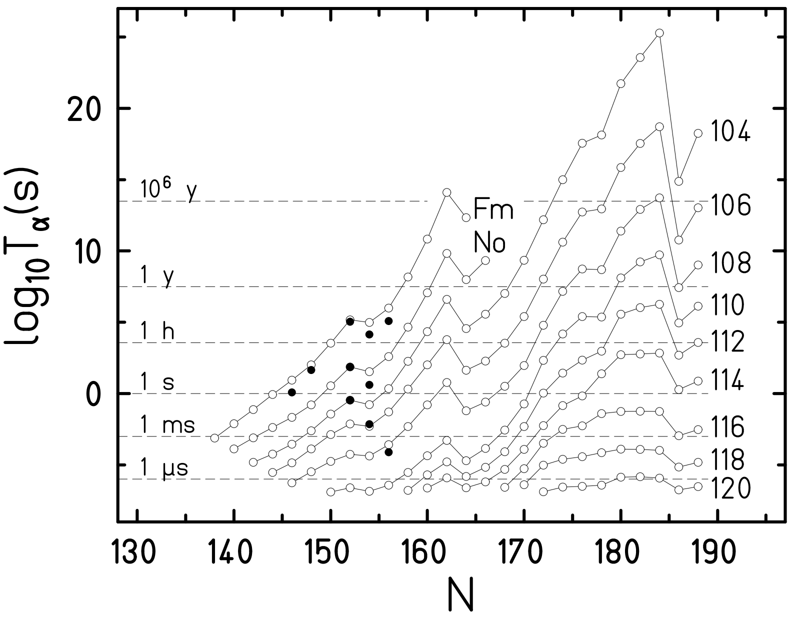

Fig.5. Calculated alpha–decay half–life T_α, in seconds, as a function of neutron number N, for elements 100 – 120. Experimental values for even–even nuclei are indicated by full circles [78,80–82].

According to the present calculations based on the phenomenological Viola and Seaborg formula with the parameters (2) and our alpha–decay energies, the alpha–decay half–life is smaller than 1 μs for even–even nuclei with $Z > 120$. Due to the effect of an unpaired nucleon the alpha–decay half–lives for odd–odd and odd–A isotopes of the element 121 may be comparable or even larger than those calculated for the neighbouring even–even isotopes of the element 120. Therefore, the element 121 is probably the heaviest one which may be detected at present, if it would be synthesized. It should be stressed, however, that the shell effect on the alpha–decay half–life for nuclei around the doubly magic nucleus $^{208}Pb_{126}$ is underestimated in phenomenological models, *e.g.* [83], and, therefore, the shell effect around the doubly magic nucleus $^{298}114_{184}$ may also be underestimated, giving too small values of alpha–decay half–life. Inclusion of additional local parameters in the phenomenological model for describing the alpha–decay half–lives for nuclei around $^{208}Pb_{126}$ [83,84] improves the agreement with experiment but causes the loss of generality. Moreover, there is no experimental data in the region of spherical superheavy nuclei to fit local parameters for these nuclei. We used the Viola and Seaborg formula with the parameters (2) and with our alpha–decay energies because the spherical superheavy nuclei are situated on the nuclear chart not far from the deformed ones (see Fig.2) for which it gives the right order of magnitude of the alpha–decay half–lives. Moreover, shell effects for spherical and deformed superheavy nuclei (the total shell correction energies) are comparable. Therefore, the alpha–decay half–lives obtained in the present paper for spherical superheavy nuclei may not be far from their real alpha–decay half–lives.

III.G Potential energy and fission trajectory

Fig.6 shows a contour map of the potential energy $E(\beta_2, \beta_4; \beta_6^{\rm m}, \beta_8^{\rm m})$ for the deformed nucleus $^{270}108_{162}$ and the spherical one $^{298}114_{184}$. Deformations $\beta_6^{\rm m}$ and $\beta_8^{\rm m}$ denote the values of the deformation parameters β_6 and β_8 , respectively, minimizing the potential energy at a given point (β_2, β_4).

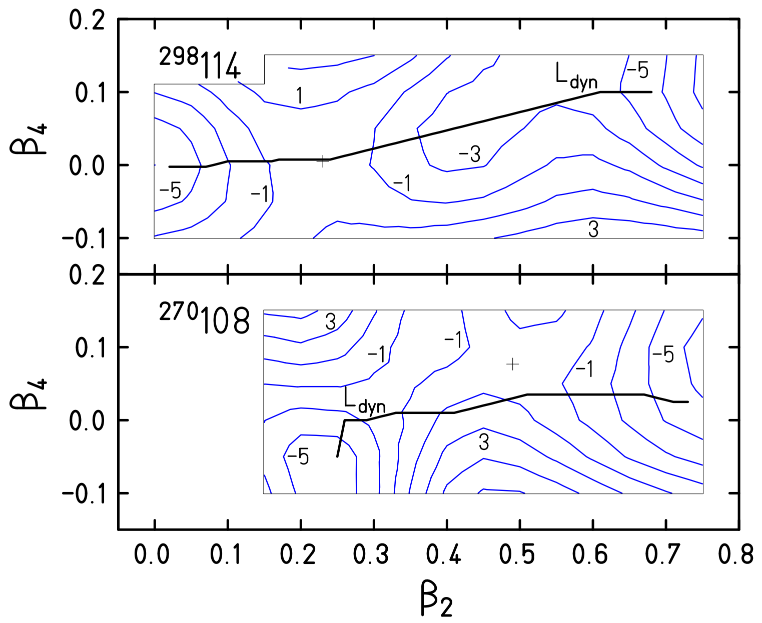

Fig.6. Contour maps of the potential energy $E(\beta_2, \beta_4; \beta_6^{\rm m}, \beta_8^{\rm m})$ for the nuclei $^{270}108_{162}$ [3] (lower part) and $^{298}114_{184}$ (upper part). The values of deformations β_6 and β_8, for which the potential energy is minimal at the point (β_2, β_4), are denoted by $\beta_6^{\rm m}$ and $\beta_8^{\rm m}$, respectively. The potential energy is calculated relative to the macroscopic energy at zero deformation. Numbers at contour lines give energy in MeV. The energy difference between the neighbouring contour lines is equal to 2 MeV. Saddle points are indicated by crosses. Dynamical $L_{\rm dyn}$ fission trajectories for both nuclei are also shown.

For these two nuclei, the dynamical fission trajectory $L_{\rm dyn}$, which minimizes the action integral, is also presented in Fig.6. It is almost horizontal, *i.e.* with constant values of β_4 in a large part of the region inside the potential energy barrier. Such dependence of β_4 on β_2 together with a rather slow variation of generally small deformations β_6 and β_8 along the fission trajectory assures small effective inertia.

For the nucleus $^{270}108_{162}$ the saddle point is located at larger quadrupole ($\beta_2^{\rm S} = 0.490$) and hexadecapole ($\beta_4^{\rm S} = 0.077$) deformations than in the case of the nucleus $^{298}114_{184}$ ($\beta_2^{\rm S} = 0.230$ and $\beta_4^{\rm S} = 0.005$). The dynamical fission trajectory $L_{\rm dyn}$ for the nucleus

$^{298}114_{184}$ goes across the saddle point because the saddle–point hexadecapole deformation β_4^{S} is very close to the equilibrium value β_4^0 .

III.H Dynamical fission barrier

Shape of the fission barrier for the nuclei $^{270}108_{162}$ and $^{298}114_{184}$, calculated along the dynamical fission trajectory L_{dyn} , is shown in Fig.7. The horizontal dashed lines indicate the energies of the fissioning nuclei. The entrance and the exit points of the barrier are located at $\beta_2^{\mathrm{en}} = 0.25$ [4] and $\beta_2^{\mathrm{ex}} = 0.73$ [4] for $^{270}108_{162}$ and at $\beta_2^{\mathrm{en}} = 0.03$ and $\beta_2^{\mathrm{ex}} = 0.68$ for $^{298}114_{184}$. The barrier heights are equal to 8.2 MeV [4] and 6.2 MeV, respectively.

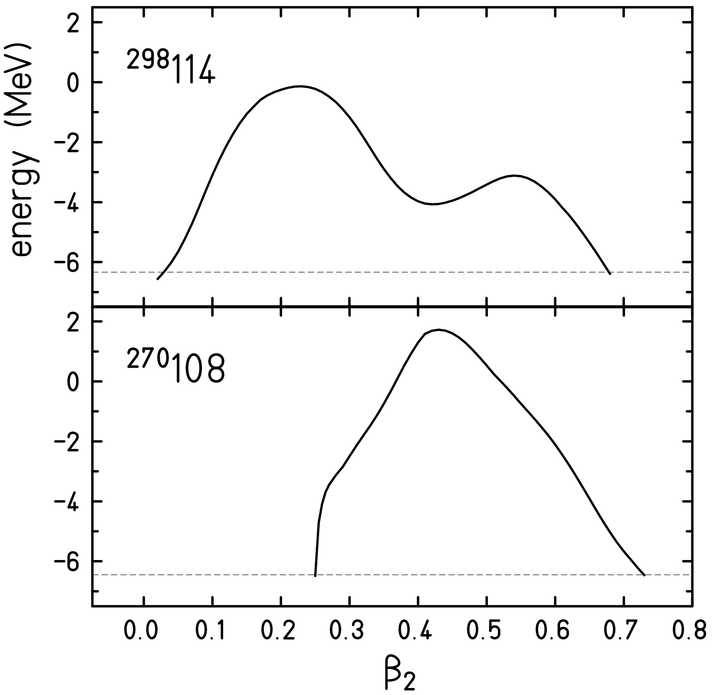

Fig.7. Dynamical fission barriers calculated for the nuclei $^{270}108_{162}$ [3] (lower part) and $^{298}114_{184}$ (upper part). The horizontal dashed lines indicate the energies of the fissioning nuclei.

The barrier obtained for $^{298}114_{184}$ is lower but considerably broader than that calculated for $^{270}108_{162}$. There is also a difference in barrier shape between $^{270}108_{162}$ and $^{298}114_{184}$. We obtained the barrier shape with two maxima for the latter nucleus in contrast to the one–maximum barrier shape for the former one. The dynamical fission trajectory and the barrier shape for the nuclei $^{270}108_{162}$ and $^{298}114_{184}$ are representative for the deformed and spherical superheavy nuclei, respectively.

Contour map of the calculated dynamical fission–barrier height $B_{\mathrm{f}}^{\mathrm{dyn}}$ for even–even nuclei with the atomic number $Z = 104 - 120$ is given in Fig.8. The shallow local maximum of $B_{\mathrm{f}}^{\mathrm{dyn}}$ with the value of 6.4 MeV is obtained for the nuclei $^{294-296}114$ and $^{296-298}116$ which are very close to the doubly magic nucleus $^{298}114_{184}$. The greatest values, exceeding

8 MeV, have been calculated in Ref.[4] for the nuclei very close to the deformed doubly magic nucleus $^{270}108_{162}$. Although the barriers calculated for the nuclei close to $^{298}114_{184}$ are lower than the ones obtained for the nuclei around $^{270}108_{162}$, they are considerably broader (cf. Table I in Ref.[4] and Table II in the present paper).

The main contribution to the barrier height $B_{\rm f}^{\rm dyn}$ comes from the total shell correction energy $E_{\rm sh}$. It is clearly seen when Fig.3 and Fig.8 are compared. These two maps are strongly correlated.

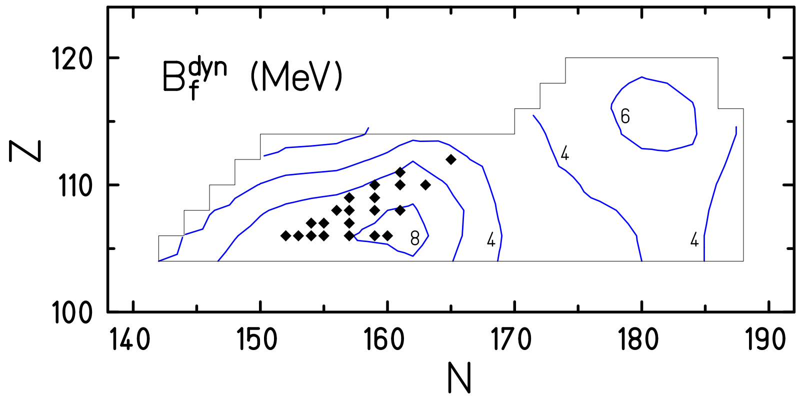

Fig.8. Contour map of the calculated dynamical fission–barrier height $B_{\rm f}^{\rm dyn}$ for even–even nuclei with the atomic number $Z = 104 - 120$. Numbers at contour lines give energy in MeV. The energy difference between neighbouring contour lines is equal to 2 MeV. Rhomb–shaped symbols denote the deformed superheavy nuclei with $Z \geq 106$ synthesized so far.

III.I Spontaneous–fission half–life

Logarithm of both spontaneous–fission and alpha–decay half–lives, calculated for isotopes of the elements $Z = 104 - 120$, is given in Fig.9. The experimental values [23,33,80–82,85] for deformed superheavy nuclei are indicated by full symbols. The detailed comparison of experimental data [23,80–82,85–89,78] to our theoretical values of the decay properties of transcalifornium nuclei has been done in Refs.[4,5].

We obtained large spontaneous–fission half–lives for nuclei close to $^{270}108_{162}$ and still much larger ones for nuclei around $^{298}114_{184}$. The local maxima of the spontaneous–fission half–life $T_{\rm sf}$ at $N = 162$ are seen. They are a consequence of the deformed neutron shell at this number. The much higher maxima of $T_{\rm sf}$ at the spherical neutron magic number $N = 184$ indicate enhanced fission stability of spherical superheavy nuclei. This is due to the considerably broader barriers and larger effective inertia obtained for them in comparison to those calculated for deformed superheavy nuclei around $^{270}108_{162}$, although the latter ones have higher barriers (see Fig.8). For the spherical doubly magic nucleus $^{298}114_{184}$ we obtain the value of $4.4 \cdot 10^5$ y for $T_{\rm sf}$. The largest value of $3.1 \cdot 10^7$ y for $T_{\rm sf}$

is calculated for the nucleus $^{288}104_{184}$ with the closed spherical neutron shell at $N = 184$. For deformed superheavy nuclei very close to the nucleus $^{270}108_{162}$, the values of the order of 1 s – 1 h for $T_{\rm sf}$ have been obtained in Ref.[4].

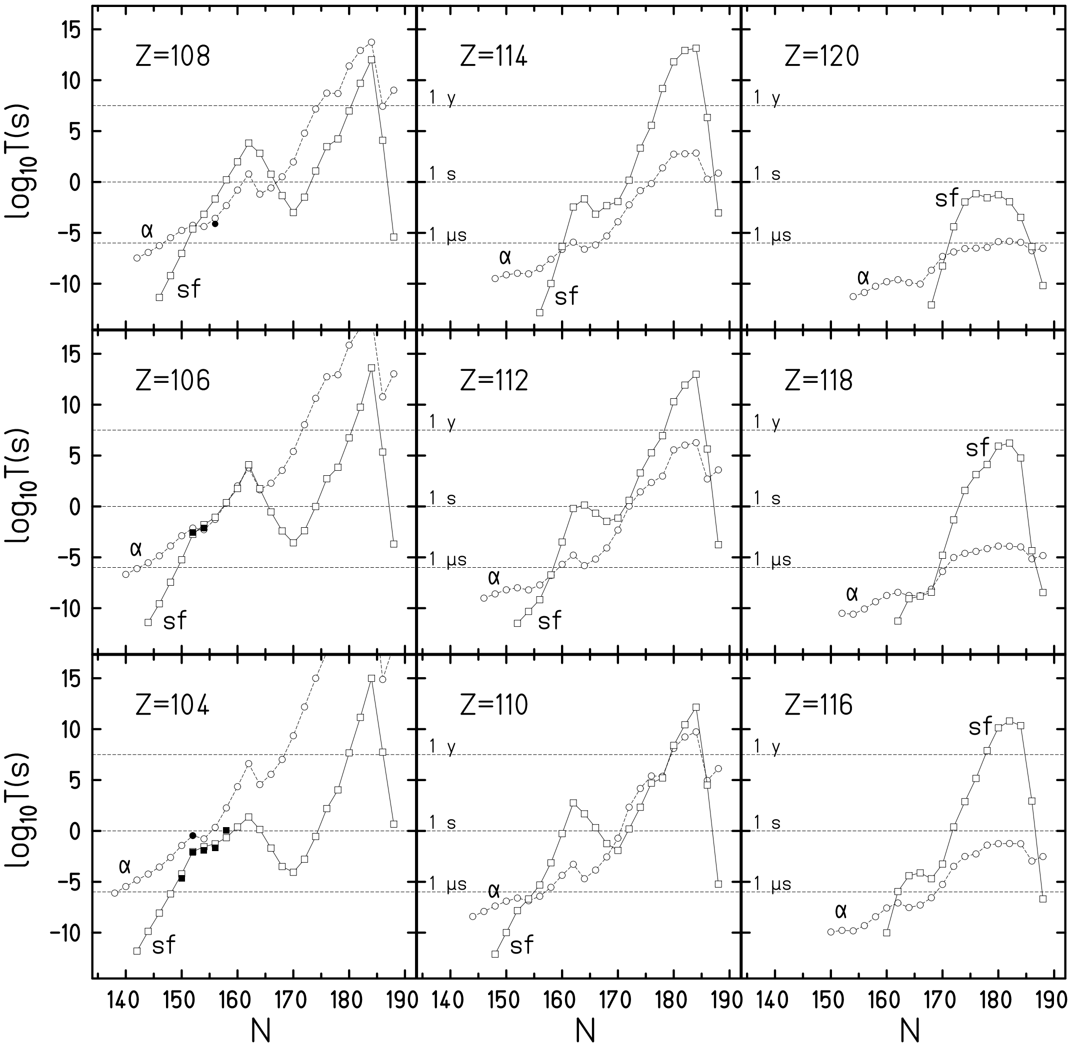

Fig.9. Dependence of logaritm of the calculated spontaneous–fission (sf) and alpha–decay (α) half–lives, given in seconds, on neutron number N, for the elements $104 - 120$. Experimental values [23,33,80–82,85] are indicated by full symbols.

Spontaneous fission limits the area of spherical superheavy nuclei to those with neutron numbers exceeding slightly the magic number $N = 184$. The nuclei $^{292}104_{188}$, $^{294}106_{188}$, $^{296}108_{188}$, $^{298}110_{188}$, $^{300}112_{188}$, $^{302}114_{188}$, $^{302}116_{186}$, $^{304}118_{186}$ and $^{304}120_{184}$ are the heaviest even–even isotopes of the elements $Z = 104 - 120$ living longer than 1 μs.

According to the present calculations, we expect that for each even–even spherical isotope of the elements $104 - 108$ the alpha–decay half–life T_α is much larger than the corresponding spontaneous–fission half–life $T_{\rm sf}$ and, therefore, for almost all even–even spherical isotopes of these elements the alpha decay should not be observed. For even–even spherical isotopes of the element 110, $T_{\rm sf}$ is comparable to T_α except the nucleus

$^{298}110_{188}$. $T_{\rm sf}$ calculated for the latter is many orders of magnitude smaller than its T_α . For almost all even–even spherical nuclei with $Z = 112 - 120$ living longer than 1 μs the spontaneous fission should not be observed. The exceptions are the nuclei $^{300}112_{188}$, $^{302}114_{188}$ and $^{304}118_{186}$. For the two former nuclei we calculate the alpha–decay half–lives much larger than the corresponding spontaneous–fission half–lives and we expect that the latter nucleus will decay by the spontaneous fission or by emission of the alpha–particle with about equal probability.

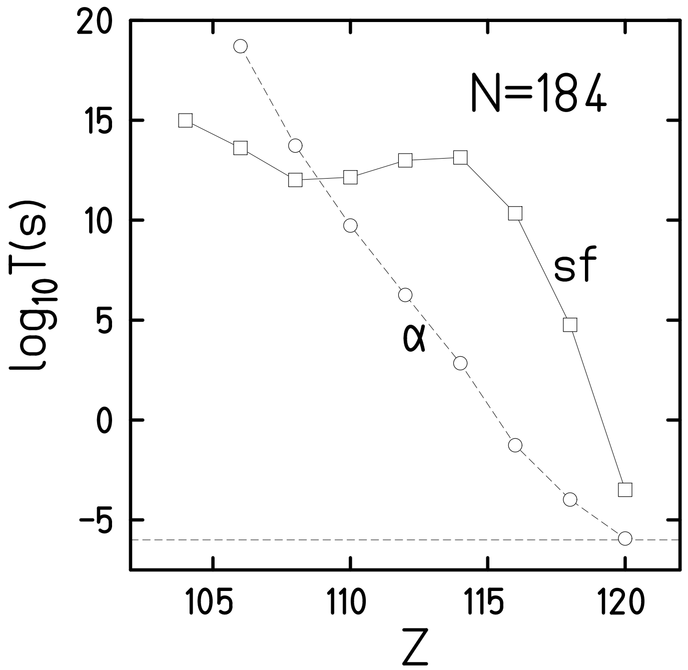

Fig.10. Dependence of logarithm of both the calculated spontaneous–fission and alpha–decay half–lives, given in seconds, on proton number Z, for isotones with the neutron number 184. The horizontal dashed line indicates the smallest nuclear half–life equal to 1 μs which can be measured in a present–day set–up after the synthesis of a superheavy nucleus.

Shell stabilization at $N = 184$ and $Z = 114$ leads to the increase of the spontaneous–fission half–life for nuclei close to $^{298}114_{184}$. The spontaneous–fission half–lives for isotopes of the element 114 with the neutron number close to 184 are larger than those obtained for corresponding isotopes of the element 112 and the latter ones are larger than the ones calculated for coresponding nuclei with $Z = 110$, because of the influence of the shell at $Z = 114$. The effect of the proton shell at $Z = 114$ in the spherical superheavy nuclei is responsible for the failure of the simple rule stating that the spontaneous–fission half–life decreases with increasing atomic number Z due to the increase of the Coulomb repulsion. It is shown in Fig.10 on the example of isotones with the neutron number 184.

The properties discussed above for even–even nuclei with the atomic number $Z = 104 - 120$, excluding the nuclei investigated in Ref.[4], are collected in Table II. Only the results for nuclei with both calculated alpha–decay and spontaneous–fission half–lives greater than 0.1 μs are given. According to the results listed in Table II and shown in Fig.9, many superheavy nuclei might be stored for a long time, if they were synthesized. For example, the total half–life calculated for the bata–stable nucleus $^{292}110_{182}$ is equal to 51 years. The total half–lives obtained for many beta–stable even–even isotopes of the elements $Z = 104 - 114$ are larger than 1 second while the even–even nuclei with larger atomic number Z are expected to live shorter than 1 second. This means that due to the effect of an unpaired nucleon the investigations of chemical properties of elements up to $Z = 115$ should be possible, if they were produced in experiment. The synthesis of these elements would open unique possibilities for atomic physics and chemistry which have at disposal large experimental and theoretical basis.

III.J Sensitivity of the obtained results to various factors

For the nuclei listed in Table I oblate minima ($\beta_2^0 < 0$) of the potential energy are lower than the prolate ($\beta_2^0 > 0$) or spherical ($\beta_2^0 \cong 0$) ones. In spite of this fact we calculate the energy of a fissioning nucleus relative to the prolate (or spherical) minimum to obtain a lower value of the spontaneous–fission half–life. The increase of the equilibrium energy (the decrease of the fission barrier) by 0.10 MeV decreases the spontaneous–fission half–life for spherical superheavy nuclei usually by $0.65 - 0.80$ orders of magnitude.

Alpha–decay energy is calculated between prolate (or spherical) minima of the decaying nucleus and its daughter nucleus. The increase (decrease) of the alpha–decay energy by 0.10 MeV decreases (increases) the alpha–decay half–life for the nucleus $^{288}104_{184}$ by about 0.95 orders of magnitude. The same increase (decrease) of the alpha–decay energy decreases (increases) the alpha–decay half–lives for spherical isotopes of the element 120 only by about 0.2 orders of magnitude.

The increase of the average zero–point vibration energy per one degree of freedom by 0.1 MeV decreases the fission barrier by the same value and, consequently, decreases the spontaneous–fission half–life usually by $0.65 - 0.80$ orders of magnitude. The alpha–decay energy and alpha–decay half–life remain unchanged because we applied the same value of the zero–point vibration energy for all considered nuclei. However, a possible significant increase of the zero–point vibration energy for the spherical doubly magic nucleus $^{298}114_{184}$ would lead to the considerably smaller stability of this nucleus against alpha decay which is expected to be its only one ground–state decay mode. The increase of the total zero–

point vibration energy by 1 MeV for the nucleus $^{298}114_{184}$ would decrease its alpha–decay half–life by about three orders of magnitude.

IV. CONCLUSIONS

Below we summarize the main conclusions of the present study.

(1) The energy gaps equal to 2.1 MeV in the proton single–particle–energy spectrum between $Z = 114$ and 115 and in the neutron spectrum between $N = 184$ and 185 are obtained for the spherical doubly magic superheavy nucleus $^{298}114_{184}$. These gaps are 1.5 times larger than the corresponding ones between $Z = 108$ and 109 and between $N = 162$ and 163 calculated for the deformed doubly magic superheavy nucleus $^{270}108_{162}$ ($^{270}\mathrm{Hs}_{162}$).

(2) The large negative total shell correction energy E_{sh} , which is responsible for the stabilization of superheavy nuclei, is about equal for the ones close to the both spherical and deformed doubly magic superheavy nuclei.

(3) The nuclei $^{264-274}104$, $^{268-280}106$, $^{276-286}108$, $^{282-292}110$, $^{288-298}112$, $^{294-302}114$ and $^{300-304}116$ are expected to be beta–stable.

(4) The dynamical fission barriers calculated for the spherical superheavy nuclei are lower but considerably broader than those obtained for the deformed ones. There is also a difference in barrier shape between the spherical and deformed superheavy nuclei. The one–maximum barrier shape is obtained for the deformed superheavy nuclei but the spherical ones have barriers with two maxima.

(5) The largest value of $3.1 \cdot 10^7$ y for the spontaneous–fission half–life T_{sf} is obtained for the nucleus $^{288}104_{184}$ with the neutron number $N = 184$ at which the spherical neutron shell is expected. For the spherical doubly magic nucleus $^{298}114_{184}$ the value of $4.4 \cdot 10^5$ y for T_{sf} is calculated. These values are much larger than the ones of the order of 1 s – 1 h obtained for T_{sf} for deformed superheavy nuclei very close to the deformed doubly magic nucleus $^{270}108_{162}$ ($^{270}\mathrm{Hs}_{162}$). The large difference in the spontaneous–fission half–life between the spherical and deformed superheavy nuclei is due to the larger effective inertia and considerably broader barriers obtained for the spherical superheavy nuclei.

(6) For the spherical doubly magic superheavy nucleus $^{298}114_{184}$, the value of 12 m for the alpha–decay half–life T_α , which is equal to the total half–life for this nucleus, is obtained. This value is not so much larger than the one of 6 s for T_α calculated for the deformed doubly magic superheavy nucleus $^{270}108_{162}$ ($^{270}\mathrm{Hs}_{162}$). However, possible

significant increase of the zero–point vibration energy for the doubly magic nucleus $^{298}114_{184}$ may considerably decrease its T_α. The increase of the total zero–point vibration energy by 1 MeV for this nucleus decreases its T_α by about three orders of magnitude.

(7) Among the even–even spherical superheavy nuclei living longer than 1 μs, $T_{\rm sf}$ is much smaller than T_α for nuclei with $Z = 104 - 108$, as well as for $^{298}110_{188}$, $^{300}112_{188}$ and $^{302}114_{188}$. For even–even spherical isotopes of the element 110 and also for the nucleus $^{304}118_{186}$, $T_{\rm sf} \approx T_\alpha$. For the remaining even–even spherical nuclei with $Z = 112 - 120$, $T_{\rm sf}$ is much larger than T_α .

(8) Calculations described in this paper lead to the conclusion that many superheavy nuclei might be stored for a long time, if they were synthesized. For example, the total half–life calculated for the beta–stable nucleus $^{292}110_{182}$ is equal to 51 years.

(9) The total half–lives obtained for many beta–stable even–even isotopes of the elements $Z = 104 - 114$ are larger than 1 second while the even–even nuclei with larger atomic number Z are expected to live shorter than 1 second. This means that due to the effect of an unpaired nucleon investigations of chemical properties of elements up to $Z = 115$ after their synthesis should be possible.

(10) The heaviest atomic nuclei possible to detect in a present–day experimental set–up, *i.e.* those living longer than 1 μs, are probably the nuclei with $Z = 121$ and N close to 184.

(11) The heaviest even–even isotopes of the elements $Z = 104 - 120$ possible to detect presently after their synthesis are the nuclei $^{292}104_{188}$, $^{294}106_{188}$, $^{296}108_{188}$, $^{298}110_{188}$, $^{300}112_{188}$, $^{302}114_{188}$, $^{302}116_{186}$, $^{304}118_{186}$ and $^{304}120_{184}$.

ACKNOWLEDGEMENT

Special thanks are due to Janusz Skalski for many valuable discussions. Support by the Polish Committee for Scientific Research (KBN) through Grant No. 2 P03B 156 08 is gratefully acknowledged.

References

[1] R. Smolańczuk, H.V. Klapdor–Kleingrothaus and A. Sobiczewski, Acta Phys. Pol. **B24** (1993) 685

[2] A. Sobiczewski, R. Smolańczuk and J. Skalski, in *Proceedings of the International Conference on Actinides–93*, Santa Fe, USA, 1993; J. Alloys Comp. **213/214** (1994) 38

[3] R. Smolańczuk, J. Skalski and A. Sobiczewski, in *Tours Symposium on Nuclear Physics II*, Tours, France, 1994, edited by H. Utsunomiya, M. Ohta, J. Galin and G. Münzenberg (World Scientific, Singapore, 1995), p.372

[4] R. Smolańczuk, J. Skalski and A. Sobiczewski, Phys. Rev. **C52** (1995) 1871

[5] R. Smolańczuk and A. Sobiczewski, in *Proceedings of XV Nuclear Physics Divisional Conference "Low Energy Nuclear Dynamics"*, St. Petersburg, Russia, 1995, edited by Yu. Oganessian, R. Kalpakchieva and W. von Oertzen (World Scientific, Singapore, 1995), p.313

[6] R. Smolańczuk, J. Skalski and A. Sobiczewski, in *Proceedings of the International Workshop XXIV on Gross Properties of Nuclei and Nuclear excitations "Extremes of Nuclear Structure"*, Hirschegg, Austria, 1996, edited by H. Feldmeier, J. Knoll and W. Nörenberg, (GSI, Darmstadt, 1996), p.35

[7] P. Möller and J.R. Nix, Nucl. Phys. **A549** (1992) 84

[8] P. Möller and J.R. Nix, in *Proceedings of the International Conference on Actinides–93*, Santa Fe, USA, 1993; J. Alloys Comp. **213/214** (1994) 43

[9] P. Möller, J.R. Nix, W.D. Myers and W.J. Swiatecki, At. Data Nucl. Data Tables **59** (1995) 185

[10] S. Ćwiok and A. Sobiczewski, Z. Phys. **A342** (1992) 203

[11] S. Ćwiok, S. Hofmann and W. Nazarewicz, Nucl. Phys. **A573** (1994) 356

[12] A. Staszczak, Z. Łojewski, A. Baran, B. Nerlo–Pomorska and K. Pomorski, in *Proceedings of the International Conference on Dynamical Aspects of Nuclear Fission*, Casta–Papiernicka, Slovakia, 1996, in print

[13] R.R. Chasman and I. Ahmad, Phys. Lett. **B392** (1997) 255

[14] R.A. Gherghescu, Z. Patyk and A. Sobiczewski, Acta Phys. Pol. **B28**, 31 (1997).

[15] R.A. Gherghescu, Z. Patyk, J. Skalski and A. Sobiczewski, in *Proceedings of the International Workshop on Research with Fission Fragments*, Benediktbeuern near Munich, Germany, 1996, in print.

[16] Y. Aboussir, J.M. Pearson, A.K. Dutta and F. Tondeur, At. Data Nucl. Data Tables **61** (1995) 127

[17] C.–L. Wu, M. Guidry and D.H. Feng, Phys. Lett. **B387** (1996) 449

[18] R. Smolańczuk and J. Dobaczewski, Phys. Rev. **C48** (1993) R2166

[19] J.–F. Berger, L. Bitaud, J. Decharge, M. Girod and S. Peru–Desenfants, in *Proceedings of the International Workshop XXIV on Gross Properties of Nuclei and Nuclear excitations "Extremes of Nuclear Structure"*, Hirschegg, Austria, 1996, edited by H. Feldmeier, J. Knoll and W. Nörenberg, (GSI, Darmstadt, 1996), p.43

[20] S. Ćwiok, J. Dobaczewski, P.–H. Heenen, P. Magierski and W. Nazarewicz, Nucl. Phys. **A611** (1996) 211

[21] G.A. Lalazissis, M.M. Sharma, P. Ring and Y.K. Gambhir, Nucl. Phys. **A608** (1996) 202

[22] R.W. Lougheed, K.J. Moody, J.F. Wild, E.K. Hulet, J.H. McQuaid, Yu.A. Lazarev, Yu.V. Lobanov, Yu.Ts. Oganessian, V.K Utyonkov, F.Sh. Abdullin, G.V. Buklanov, B.N. Gikal, S. Iliev, A.N. Mezentsev, A.N. Polyakov, I.M. Sedykh, I.V. Shirokovsky, V.G. Subbotin, A.M. Sukhov, Yu.S. Tsyganov and V.E.Zhuchko, in *Proceedings of the International Conference on Actinides–93*, Santa Fe (USA), 1993; J. Alloys Comp. **213/214** (1994) 61

[23] Yu.A. Lazarev, Yu.V. Lobanov, Yu.Ts. Oganessian, V.K. Utyonkov, F.Sh. Abdullin, G.V. Buklanov, B.N. Gikal, S. Iliev, A.N. Mezentsev, A.N. Polyakov, I.M. Sedykh, I.V. Shirokovsky, V.G. Subbotin, A.M. Sukhov, Yu.S. Tsyganov, V.E. Zhuchko, R.W. Lougheed, K.J. Moody, J.F. Wild, E.K. Hulet and J.H. McQuaid, Phys. Rev. Lett. **73** (1994) 624

[24] Yu.A. Lazarev, Yu.Ts. Oganessian, Yu.S. Tsyganov, V.K. Utyonkov, F.Sh. Abdullin, S. Iliev, A.N. Polyakov, J. Rigol, I.V. Shirokovsky, V.G. Subbotin, A.M. Sukhov, G.V. Buklanov, B.N. Gikal, V.B. Kutner, A.N. Mezentsev, I.M. Sedykh, D.V. Vakatov, R.W. Lougheed, J.F. Wild, K.J. Moody and E.K. Hulet Phys. Rev. Lett. **75** (1995) 1903

[25] Yu.A. Lazarev, in *Proceedings of XV Nuclear Physics Divisional Conference "Low Energy Nuclear Dynamics"*, St. Petersburg, Russia, 1995, edited by Yu. Oganessian, R. Kalpakchieva and W. von Oertzen (World Scientific, Singapore, 1995), p.293

[26] Yu.A. Lazarev, Yu.V. Lobanov, Yu.Ts. Oganessian, V.K. Utyonkov, F.Sh. Abdullin, A.N. Polyakov, J. Rigol, I.V. Shirokovsky, Yu.S. Tsyganov, S. Iliev, V.G. Subbotin, A.M. Sukhov, G.V. Buklanov, B.N. Gikal, V.B. Kutner, A.N. Mezentsev, K. Subotic, J.F. Wild, R.W. Lougheed and K.J. Moody, Phys. Rev. **C54** (1996) 620

[27] Yu.A. Lazarev, in *Proceedings of the International Workshop XXIV on Gross Properties of Nuclei and Nuclear excitations "Extremes of Nuclear Structure"*, Hirschegg, Austria, 1996, edited by H. Feldmeier, J. Knoll and W. Nörenberg, (GSI, Darmstadt, 1996), p.11

[28] S. Hofmann, V. Ninov, F.P. Hessberger, P. Armbruster, H. Folger, G. Münzenberg, H.J. Schött, A.G. Popeko, A.V. Yeremin, A.N. Andreyev, S. Saro, R. Janik and M. Leino, Z. Phys. **A350** (1995) 277

[29] S. Hofmann, GSI–Nachrichten 02–95

[30] S. Hofmann, V. Ninov, F.P. Hessberger, P. Armbruster, H. Folger, G. Münzenberg, H.J. Schött, A.G. Popeko, A.V. Yeremin, A.N. Andreyev, S. Saro, R. Janik and M. Leino, Z. Phys. **A350** (1995) 281

[31] S. Hofmann, V. Ninov, F.P. Hessberger, P. Armbruster, H. Folger, G. Münzenberg, H.J. Schött, A.G. Popeko, A.V. Yeremin, S. Saro, R. Janik and M. Leino, Z. Phys. **A354** (1996) 229

[32] F.P. Hessberger, in *Proceedings of the International Workshop XXIV on Gross Properties of Nuclei and Nuclear excitations "Extremes of Nuclear Structure"*, Hirschegg, Austria, 1996, edited by H. Feldmeier, J. Knoll and W. Nörenberg, (GSI, Darmstadt, 1996), p.1

[33] F.P. Hessberger, S. Hofmann, V. Ninov, P. Armbruster, H. Folger, G. Münzenberg, A.G. Popeko, A.V. Yeremin, A.N. Andreyev, S. Saro and M. Leino, GSI Scientific Report 1995 (Report GSI 96–1, Darmstadt 1996), p.9

[34] A. Ghiorso, D. Lee, L.P. Somerville, W. Loveland, J.M. Nitschke, W. Ghiorso, G.T. Seaborg, P. Wilmarth, R. Leres, A. Wydler, M. Nurmia, K. Gregorich, K. Czerwinski, R. Gaylord, T. Hamilton, N.J. Hannink, D.C. Hoffman, C. Jarzynsky, C. Kacher, B. Kadkhodayan, S. Kreek, M. Lane, A. Lyon, M.A. McMahan, M. Neu, T. Sikkeland, W.J. Swiatecki, A. Türler, J.T. Walton and S. Yashita, Phys. Rev. **C51** (1995) R2293

[35] D.C. Hoffman and M.R. Lane, Radiochimica Acta **70/71** (1995) 135

[36] M.R. Lane, K.E. Gregorich, D.M. Lee, M.F. Mohar, M. Hsu, C.D. Kacher, B. Kadkhodayan, M.P. Neu, N.J. Stoyer, E.R. Sylwester, J.C. Yang and D.C. Hoffman, Phys. Rev. **C53** (1996) 2893

[37] Z. Patyk, A. Sobiczewski, P. Armbruster and K.–H. Schmidt, Nucl. Phys. **A491** (1989) 267

[38] Z. Patyk, R. Smolańczuk and A. Sobiczewski, GSI Scientific Report 1990 (Report GSI 91–1, Darmstadt 1991), p.79

[39] Z. Patyk and A. Sobiczewski, Phys. Lett. **B256** (1991) 207

[40] Z. Patyk and A. Sobiczewski, Nucl. Phys. **A533** (1991) 132

[41] M. Schädel *et al.*, GSI Scientific Report 1995 (Report GSI 96–1, Darmstadt 1996), p.10

[42] S. Bjørnholm and J.E. Lynn, Rev. Mod. Phys. **52** (1980) 725

[43] V.E. Viola Jr. and G.T. Seaborg, J. Inorg. Nucl. Chem. **28** (1966) 741

[44] S. Hofmann, in *Proceedings of the International Conference on Actinides–93*, Santa Fe, USA, 1993; J. Alloys Comp. **213/214** (1994) 74

[45] H.C. Pauli, Phys. Reports **7C** (1973) 35; Nukleonika **20** (1975) 601

[46] A. Baran, K. Pomorski, A. Lukasiak and A. Sobiczewski, Nucl. Phys. **A361** (1981) 83

[47] M. Brack, J. Damgaard, A.S. Jensen, H.C. Pauli, V.M. Strutinsky and C.Y. Wong, Rev. Mod. Phys. **44** (1972) 320

[48] K.H. Böning, Z. Patyk, A. Sobiczewski and S. Ćwiok, Z. Phys. **A325** (1986) 479

[49] A. Sobiczewski, Z. Patyk and S. Ćwiok, Phys. Lett. **B186** (1987) 6

[50] P. Möller, J.R. Nix and W.J. Swiatecki, Nucl. Phys. **A469** (1987) 1

[51] P. Möller, J.R. Nix and W.J. Swiatecki, Nucl. Phys. **A492** (1989) 349

[52] A. Sobiczewski and R. Smolańczuk, Acta Phys. Pol. **B27** (1996) 1011

[53] G. Audi and A.H. Wapstra, Nucl. Phys. **A565** (1993) 1

[54] P. Möller and J.R. Nix, At. Data Nucl. Data Tables **26** (1981) 165

[55] Z. Patyk, J. Skalski, A. Sobiczewski and S. Ćwiok, Nucl. Phys. **A502** (1989) 591c

[56] A. Sobiczewski, F.A. Gareev and B.N. Kalinkin, Phys. Lett. **22** (1966) 500

[57] H. Meldner, Ark. Fys. **36** (1967) 593

[58] H.F. Boersma, Phys. Rev. **C48** (1993) 472

[59] J. Dobaczewski, H. Flocard and J. Treiner, Nucl. Phys. **A422** (1984) 103

[60] J. Dechargé and D. Gogny, Phys. Rev. **C21** (1980) 1568

[61] S.G. Nilsson, J.R. Nix, A. Sobiczewski, Z. Szymański, S. Wycech, C. Gustafson and P. Möller, Nucl. Phys. **A115** (1968) 545

[62] S.G. Nilsson, Chin Fu Tsang, A. Sobiczewski, Z. Szymański, S. Wycech, C. Gustafson, I.–L. Lamm, P. Möller and B. Nilsson, Nucl. Phys. **A131** (1969) 1

[63] A. Łukasiak, A. Sobiczewski and W. Stępień–Rudzka, Acta Phys. Pol. **B2** (1971) 535

[64] E.O. Fiset and J.R. Nix, Nucl. Phys. **A193** (1972) 647

[65] J. Randrup, S.E. Larsson, P. Möller, A. Sobiczewski and A. Łukasiak, Phys. Scr. **10A** (1974) 60

[66] F. Tondeur, Z. Phys. **A288** (1978) 97

[67] P. Armbruster, Annu. Rev. Nucl. Part. Sci. **35** (1985) 135

[68] Yu.Ts. Oganessian, JINR Preprint E7–96–434, Dubna, 1996

[69] D. Habs, in *Proceedings of the International Workshop on Research with Fission Fragments*, Benediktbeuern near Munich, Germany, 1996, in print

[70] R. Smolańczuk, in *Proceedings of the International Conference on Dynamical Aspects of Nuclear Fission*, Casta–Papiernicka, Slovakia, 1996, in print

[71] A. Sobiczewski, Z. Patyk, S. Ćwiok and P. Rozmej, Nucl. Phys. **A485** (1988) 16

[72] P.A. Butler and W. Nazarewicz, Rev. Mod. Phys. **68** (1996) 349

[73] R. Smolańczuk, J. Skalski and A. Sobiczewski, in *Proceedings of the International School–Seminar on Heavy Ion Physics*, Dubna, Russia, 1993, edited by Yu.Ts. Oganessian, Yu.E. Penionzhkevich and R. Kalpakchieva (JINR, Dubna, 1993), Vol.1, p.157

[74] R.A. Gherghescu, J. Skalski, Z. Patyk and A. Sobiczewski, an article in preparation

[75] L.–O Jönsson, Nucl.Phys. **A608** (1996) 1

[76] V.M. Strutinsky, Nucl. Phys. **A95** (1967) 420; **A122** (1968) 1

[77] S. Ćwiok, J. Dudek, W. Nazarewicz, J. Skalski and T. Werner, Comput. Phys. Commun. **46** (1987) 379

[78] B. Buck, A.C. Merchant and S.M. Perez, At. Data Nucl. Data Tables **54** (1993) 53

[79] A. Sobiczewski, Z. Patyk and S. Ćwiok, Phys. Lett. **B224** (1989) 1

[80] F.P. Hessberger, G. Münzenberg, S. Hofmann, W. Reisdorf, K.H. Schmidt, H.J. Schött, P. Armbruster, R. Hingmann, B. Thuma and D. Vermeulen, Z. Phys. **A321** (1985) 317

[81] G. Münzenberg, S. Hofmann, H. Folger, F.P. Hessberger, J. Keller, K. Poppensieker, B. Quint, W. Reisdorf, K.H. Schmidt, H.J. Schött, P. Armbruster, M.E. Leino and R. Hingmann, Z. Phys. **A322** (1985) 227

[82] G. Münzenberg, P. Armbruster, G. Berthes, H. Folger, F.P. Hessberger, S. Hofmann, K. Poppensieker, W. Reisdorf, B. Quint, K.H. Schmidt, H.J. Schött, K. Sümmerer, I. Zychor, M.E. Leino, U. Gollerthan and E. Hanelt, Z. Phys. **A324** (1986) 489

[83] Y. Hatsukawa, H. Nakahara and D.C. Hoffman, Phys. Rev. **C42** (1990) 674

[84] J. Dechargé and L. Pangault, Rapport CEA–R–5672, Centre d'Etudes de Bruyères–le–Châtel, 1994

[85] L.P. Somerville, M.J. Nurmia, J.M. Nitschke, A. Ghiorso, E.K. Hulet and R.W. Lougheed, Phys. Rev. **C31** (1985) 1801

[86] G.M. Ter-Akopyan, A.S. Iljinov, Yu.Ts. Oganessian, O.A. Orlova, G.S. Popeko, S.P. Tretyakova, V.I. Chepigin, B.V. Shilov and G.N. Flerov, Nucl. Phys. **A255** (1975) 509

[87] E.K. Hulet, R.W. Lougheed, J.F. Wild, R.J. Dougan, K.J. Moody, R.L. Hahn, C.M. Henderson, R.J. Dupzyk and G.R. Bethune, Phys. Rev. **C34** (1986) 1394

[88] E.K. Hulet, J.F. Wild, R.J. Dougan, R.W. Lougheed, J.H. Landrum, A.D. Dougan, P.A. Baisden, C.M. Henderson, R.J. Dupzyk, R.L. Hahn, M. Schädel, K. Sümmerer and G.R. Bethune, Phys. Rev. **C40** (1989) 770

[89] E.K. Hulet, in *Proceedings of the Robert A. Welch Foundation Conference on Chemical Research XXXIV "Fifty Years with Transuranium Elements"*, Houston, USA, 1990, p. 279.

Table I. The calculated oblate deformation energy $\mathring{E}_{\rm def}$, oblate equilibrium deformation parameter $\mathring{\beta}_2^0$ and prolate (spherical) – oblate energy difference ΔE for these superheavy nuclei which have the deeper oblate minimum and for which we calculate alpha–decay and spontaneous–fission half–lives larger than 0.1 μs.

Z –	N –	$\mathring{E}_{\rm def}$ (MeV)	$\mathring{\beta}_2^0$ –	ΔE (MeV)	Z –	N –	$\mathring{E}_{\rm def}$ (MeV)	$\mathring{\beta}_2^0$ –	ΔE (MeV)
104	174	1.36	-.125	0.05	116	170	0.50	-.112	0.11
104	176	0.94	-.106	0.09	116	172	0.50	-.112	0.09
104	178	0.74	-.099	0.47	116	174	0.34	-.090	0.03
104	180	0.16	-.057	0.11	116	176	0.20	-.078	0.10
104	182	0.04	-.042	0.01	116	178	0.04	-.065	0.02
106	178	0.64	-.098	0.34	118	170	0.72	-.116	0.20
106	180	0.13	-.052	0.07	118	172	0.74	-.116	0.13
					118	176	0.39	-.088	0.09
108	178	0.46	-.094	0.19	118	178	0.19	-.080	0.15
108	180	0.09	-.045	0.04					
					120	172	0.93	-.123	0.27
110	178	0.23	-.084	0.09	120	174	0.72	-.115	0.06
					120	176	0.45	-.098	0.06
114	176	0.07	-.075	0.01	120	178	0.22	-.088	0.19

Table II. The calculated properties corresponding to the prolate (or spherical) equilibrium shapes of nuclei specified in the first two columns for which we calculate the alpha–decay and spontaneous–fission half–lives larger than 0.1 μs.

Z	N	$E_{\rm def}$	β_2^0	$\beta_2^{\rm en}$	$\beta_2^{\rm ex}$	$B_{\rm f}^{\rm dyn}$	$E_{\rm sh}$	$\log_{10}T_{\rm sf}(s)$	M	Q_α	$\log_{10}T_\alpha(s)$
–	–	(MeV)	–	–	–	(MeV)	(MeV)		(MeV)	(MeV)	
104	170	2.53	.163	.21	.66	3.6	-3.60	-4.07	131.62	6.56	9.35
104	172	1.83	.139	.19	.67	3.4	-3.61	-2.78	137.88	6.02	12.18
104	174	1.31	.107	.16	.67	3.4	-3.85	-0.55	144.37	5.55	15.00
104	176	0.85	.092	.13	.68	3.5	-4.18	2.19	151.19	5.17	17.56
104	178	0.27	.061	.11	.68	3.6	-4.34	4.03	158.59	5.09	18.13
104	180	0.05	.032	.08	.69	4.0	-4.77	7.67	166.15	4.63	21.74
104	182	0.03	.001	.05	.71	4.3	-5.20	11.15	174.11	4.42	23.57
104	184	0.03	.001	.04	.75	4.6	-5.58	14.99	182.54	4.23	25.28
104	186	0.22	.001	.04	.71	3.3	-4.37	7.74	192.93	5.57	14.88
104	188	0.60	.004	.02	.67	2.1	-3.30	0.66	203.57	5.08	18.25
106	172	1.86	.133	.19	.67	3.3	-4.06	-2.38	141.06	7.02	8.03
106	174	1.38	.107	.16	.67	3.3	-4.30	-0.01	146.79	6.48	10.62
106	176	0.95	.087	.13	.67	3.4	-4.60	2.72	152.89	6.09	12.74
106	178	0.30	.065	.11	.67	3.6	-4.65	3.84	159.67	6.06	12.94
106	180	0.06	.029	.08	.68	4.1	-4.97	6.74	166.60	5.58	15.85
106	182	0.03	.001	.06	.69	4.4	-5.33	9.75	173.91	5.33	17.53
106	184	0.03	.001	.04	.71	4.6	-5.61	13.61	181.70	5.16	18.71
106	186	0.13	.001	.04	.67	3.3	-4.36	5.34	191.42	6.46	10.77
106	188	0.44	.002	.04	.62	2.1	-3.24	-3.70	201.39	6.04	13.03
108	174	1.33	.105	.16	.67	3.4	-4.81	1.08	150.88	7.39	7.17
108	176	0.92	.094	.13	.67	3.7	-5.08	3.47	156.26	7.05	8.73
108	178	0.27	.066	.11	.67	4.0	-5.06	4.23	162.37	7.06	8.69
108	180	0.05	.030	.08	.67	4.4	-5.35	6.98	168.60	6.51	11.40
108	182	0.03	.001	.06	.68	4.8	-5.64	9.69	175.25	6.23	12.92
108	184	0.03	.001	.03	.69	4.9	-5.82	12.01	182.41	6.08	13.73
108	186	0.04	.001	.05	.66	3.5	-4.52	4.09	191.46	7.34	7.43
108	188	0.21	.000	.05	.52	2.2	-3.31	-5.41	200.83	6.99	9.02
110	176	0.76	.088	.13	.67	4.3	-5.59	4.69	161.32	8.02	5.40
110	178	0.14	.062	.11	.67	4.5	-5.55	5.20	166.71	8.02	5.37
110	180	0.04	.018	.08	.67	4.9	-5.88	8.40	172.16	7.36	8.11
110	182	0.03	.001	.05	.68	5.2	-6.10	10.43	178.15	7.12	9.23
110	184	0.03	.001	.03	.69	5.3	-6.19	12.15	184.68	7.01	9.73
110	186	0.04	.001	.04	.65	3.9	-4.94	4.50	192.97	8.13	4.96
110	188	0.08	.001	.05	.51	2.6	-3.63	-5.23	201.72	7.84	6.12
112	176	0.39	.088	.13	.66	4.8	-5.97	5.27	168.20	9.06	2.35
112	178	0.05	.014	.10	.67	5.2	-6.15	6.95	172.62	8.87	2.98
112	180	0.05	.009	.07	.67	5.7	-6.51	10.29	177.30	8.17	5.56
112	182	0.05	.006	.05	.68	5.8	-6.67	11.92	182.63	8.05	6.02
112	184	0.04	.005	.03	.68	5.7	-6.65	12.99	188.56	7.99	6.26
112	186	0.05	.002	.04	.65	4.5	-5.46	5.64	196.07	8.96	2.70
112	188	0.08	.001	.05	.52	3.1	-4.17	-3.76	204.09	8.70	3.59

Table II. Continued.

Z	N	$E_{\rm def}$	β_2^0	$\beta_2^{\rm en}$	$\beta_2^{\rm ex}$	$B_{\rm f}^{\rm dyn}$	$E_{\rm sh}$	$\log_{10}T_{\rm sf}(s)$	M	Q_α	$\log_{10}T_\alpha(s)$
–	–	(MeV)	–	–	–	(MeV)	(MeV)		(MeV)	(MeV)	
114	176	0.06	.001	.12	.66	5.3	-6.28	5.57	176.80	10.08	-0.16
114	178	0.07	.001	.08	.67	5.9	-6.76	9.18	180.19	9.57	1.38
114	180	0.08	.001	.06	.67	6.4	-7.07	11.80	184.20	9.15	2.73
114	182	0.03	.001	.04	.68	6.4	-7.16	12.92	188.86	9.13	2.77
114	184	0.04	.001	.03	.68	6.2	-7.04	13.14	194.17	9.11	2.84
114	186	0.04	.001	.04	.65	5.0	-5.90	6.33	200.91	9.93	0.28
114	188	0.05	.001	.04	.51	3.6	-4.62	-3.04	208.22	9.73	0.87
116	168	0.70	.176	.21	.63	3.1	-5.25	-4.70	180.55	12.96	-6.57
116	170	0.39	.079	.19	.63	3.5	-5.36	-3.26	181.68	12.34	-5.26
116	172	0.41	.077	.16	.64	4.3	-5.82	0.39	182.94	11.56	-3.48
116	174	0.31	.075	.13	.65	5.1	-6.20	2.87	184.76	11.17	-2.51
116	176	0.10	.048	.12	.65	5.6	-6.47	5.16	187.16	11.07	-2.26
116	178	0.02	.001	.08	.66	6.1	-6.81	7.89	189.96	10.74	-1.40
116	180	0.02	.001	.06	.66	6.4	-7.07	10.13	193.29	10.68	-1.25
116	182	0.03	.001	.05	.66	6.4	-7.09	10.80	197.30	10.68	-1.24
116	184	0.03	.001	.03	.66	6.1	-6.88	10.34	201.97	10.69	-1.26
116	186	0.03	.001	.04	.61	4.9	-5.81	2.93	207.94	11.35	-2.96
116	188	0.04	.001	.05	.40	3.7	-4.56	-6.69	214.50	11.17	-2.52
118	170	0.52	.079	.17	.62	3.7	-5.37	-4.80	196.09	13.11	-6.39
118	172	0.61	.080	.13	.63	4.6	-5.86	-1.32	196.57	12.46	-5.02
118	174	0.56	.077	.12	.63	5.3	-6.25	1.57	197.63	12.27	-4.61
118	176	0.30	.070	.11	.64	5.7	-6.44	3.13	199.38	12.19	-4.42
118	178	0.04	.033	.09	.63	5.9	-6.56	4.12	201.66	12.07	-4.15
118	180	0.01	.005	.07	.63	6.1	-6.73	5.93	204.35	11.96	-3.90
118	182	0.01	.001	.05	.63	6.0	-6.70	6.22	207.68	11.97	-3.91
118	184	0.02	.001	.04	.62	5.7	-6.41	4.76	211.72	11.99	-3.98
118	186	0.02	.001	.04	.39	4.6	-5.40	-4.35	216.92	12.52	-5.15
120	172	0.66	.082	.13	.61	4.5	-5.59	-4.40	212.10	13.59	-6.88
120	174	0.66	.082	.12	.61	5.1	-5.99	-1.97	212.41	13.42	-6.55
120	176	0.39	.077	.11	.61	5.4	-6.14	-1.16	213.46	13.40	-6.51
120	178	0.03	.039	.09	.61	5.5	-6.10	-1.56	215.17	13.36	-6.43
120	180	0.00	.000	.07	.61	5.7	-6.22	-1.25	217.17	13.09	-5.87
120	182	0.01	.000	.05	.59	5.5	-6.14	-1.94	219.84	13.07	-5.83
120	184	0.01	.000	.04	.38	5.1	-5.79	-3.49	223.23	13.12	-5.93
120	186	0.01	.000	.04	.36	4.1	-4.81	-6.35	227.68	13.53	-6.76